

CHAPTER 4: Tube with Flat Length-to-Width Ratio of 5:1

4.1 Introduction

A tube with a flat length-to-width ratio of 5:1 was modeled. The elements used in this case are the same size as those used for the 2:1 length-to-width ratio case; the only difference is that more elements are used in order to make the tube longer. Parameters used in this study include:

Flat Length: $L_f = 7.5\text{m}$

Flat Width: $W_f = 1.5\text{m}$

Half Length: $a = 0.5L_f = 3.75\text{m}$

Half Width: $b = 0.5W_f = 0.75\text{m}$

Poisson's Ratio: $\nu = 0.45$

Thickness: $t = 3\text{mm}$

Young's Modulus: $E = 7.0346 \times 10^9 \text{ Pa}$

Specific Weight: $\gamma_{\text{slurry}} = 1.5\gamma_{\text{water}}$

One-quarter of the tube was modeled. The initial shape is shown in Figure 4.1.1. This model is studied with two different distributed spring stiffnesses, $4.20 \times 10^6 \text{ N/m}^3$ and $8.40 \times 10^4 \text{ N/m}^3$; these are the same values used in the 2:1 length-to-width ratio case described in Chapter 3.

This chapter presents the effects of hydrostatic pressure on an initially flat tube with a length-to-width ratio of 5:1. The geometry of the tube is discussed, along with the mid-surface stresses that form in the material, the amount of contact between the tube and its foundation, and the relationship between the height of the tube and the amount of hydrostatic pressure applied.

4.2 Distributed Spring Stiffness, K_d , of $4.20 \times 10^6 \text{ N/m}^3$

4.2.1 Geometry

One-quarter of the tube was modeled using tensionless springs with a distributed spring stiffness of $K_d = 4.20 \times 10^6 \text{ N/m}^3$. The maximum amount of hydrostatic pressure applied to the tube at ground level ($Z = 0$) was 10,297 Pa. This equates to a pressure head of 0.7m, such that at $Z = 0.7\text{m}$ the applied pressure is zero.

A three-dimensional plot of the model is shown in Figure 4.2.1.1. The top surface of the tube deflected upward at the center 0.472m from its initial height of 0.0429m, and the bottom surface of the tube deflected downward at the center 2.49mm from its initial height of 0.0m. The wrinkling that occurs in the tube is apparent in the figure.

Figure 4.2.1.2 shows cross-sectional plots of the tube along the X- and Y-axes. The coordinates of the tube's edge, in meters, at B_x , B_y , and the corner are (3.73, 0.0, 0.187), (0.0, 0.675, 0.211), and (3.73, 0.740, 0.195), respectively.

4.2.2 Contact Region

The contact regions for pressure heads of 0.5m and 0.7m are shown in Figure 4.2.2.1. Circles denote locations of active springs for pressure heads of 0.5m and 0.7m. Open squares signify the locations of those springs which are active for the 0.5m pressure head case, but not for a pressure head of 0.7m. There are no springs which are active for a pressure head of 0.7m but not for a pressure head of 0.5m. As expected, the contact region decreases as the pressure head increases.

Figure 4.2.2.2 shows the contact region for the entire tube when a pressure head of 0.7m is applied. The figure shows how all of the points on the edge move toward the center and the sides curve inward between the corners.

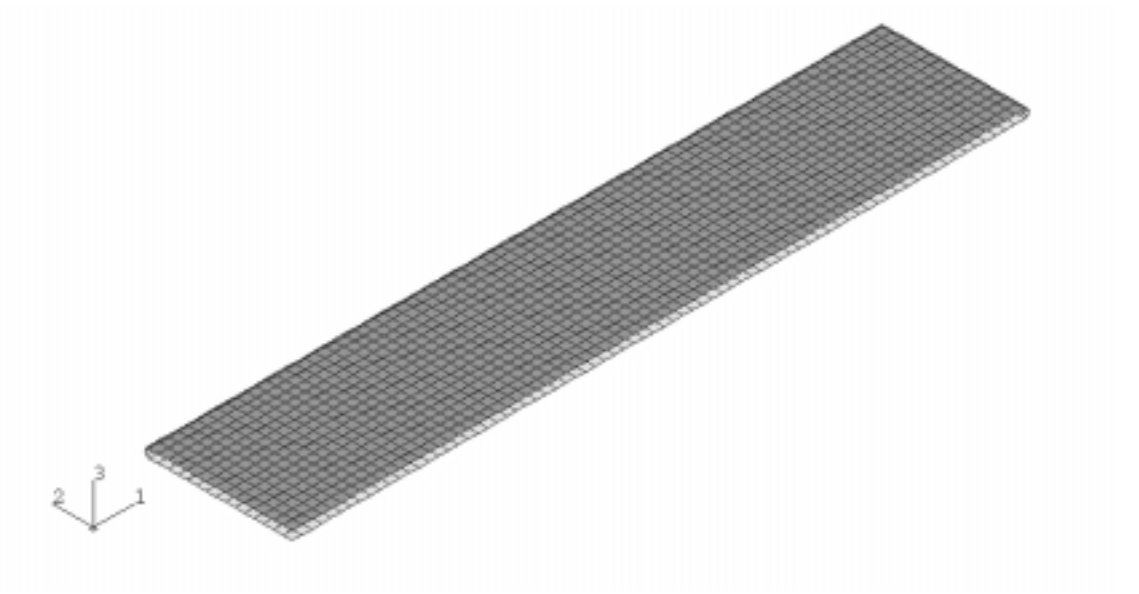


Figure 4.1.1: Initial Shape of Quarter Tube with $L_f:W_f$ of 5:1

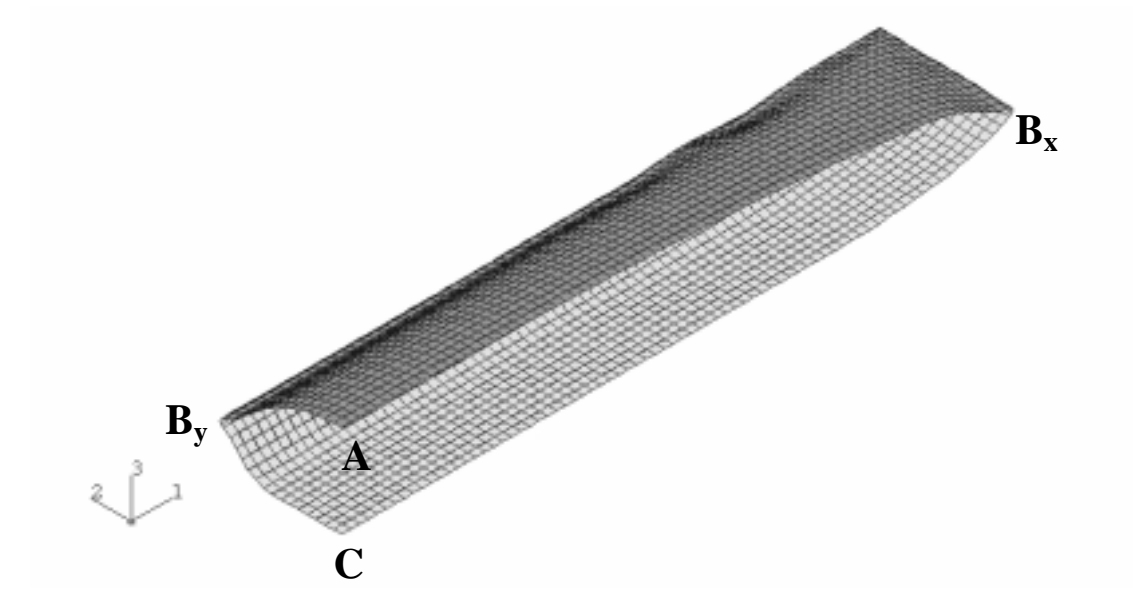
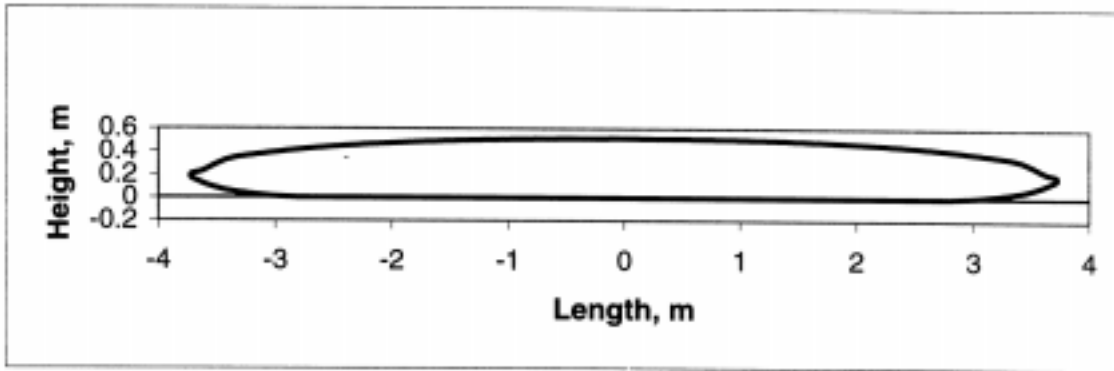
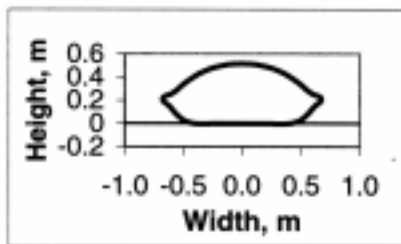


Figure 4.2.1.1: Pressure Head of 0.7m for $K_d = 4.20 \times 10^6 \text{ N/m}^3$ and $L_f:W_f$ of 5:1



a: Along X-Axis



b: Along Y-Axis

Figure 4.2.1.2: Cross Sections of the Tube at a Pressure Head of 0.7m for $K_d = 4.20 \times 10^6$ N/m^3 and $L_f:W_f$ of 5:1

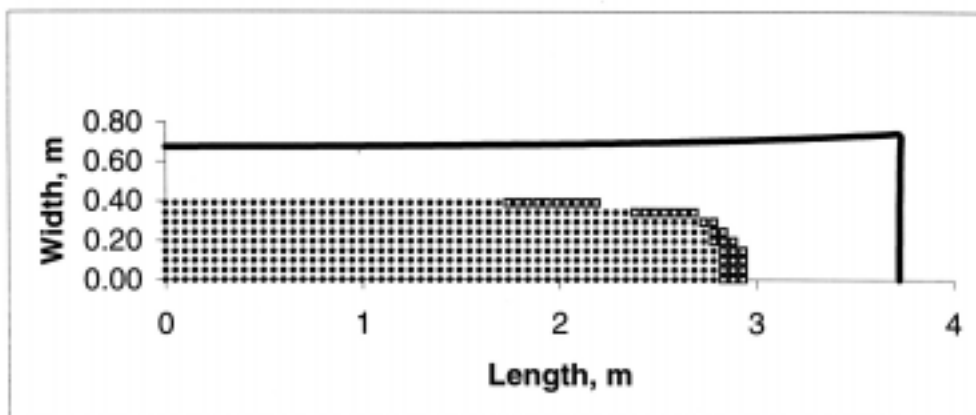


Figure 4.2.2.1: Quarter Contact Region at Pressure Heads of 0.5m and 0.7m for $K_d = 4.20 \times 10^6$ N/m^3 and $L_f:W_f$ of 5:1; circles: 0.5m and 0.7m, squares: 0.5m

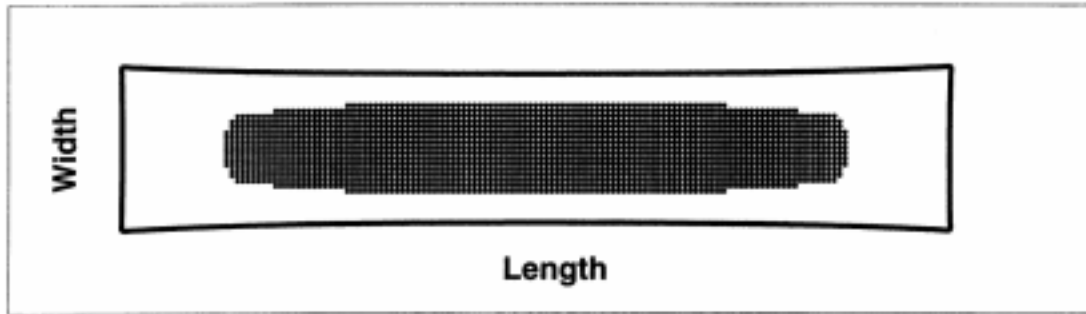


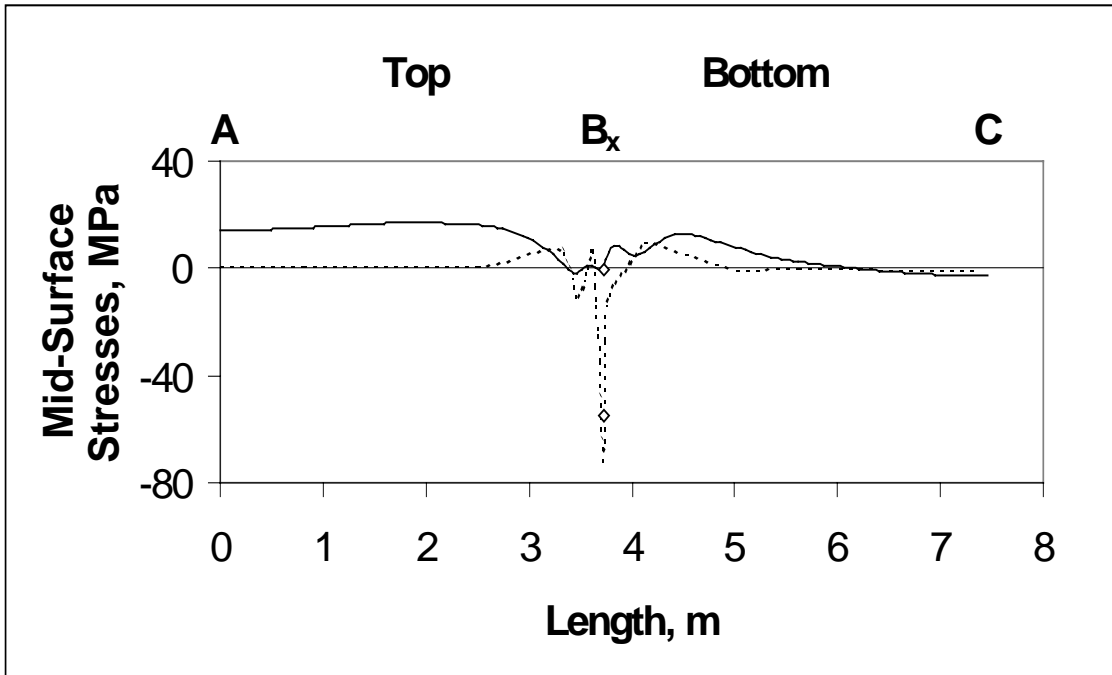
Figure 4.2.2.2: Whole Contact Region at a Pressure Head of 0.7m for $K_d = 4.20 \times 10^6$ N/m^3 and $L_f:W_f$ of 5:1

4.2.3 Mid-Surface Stresses

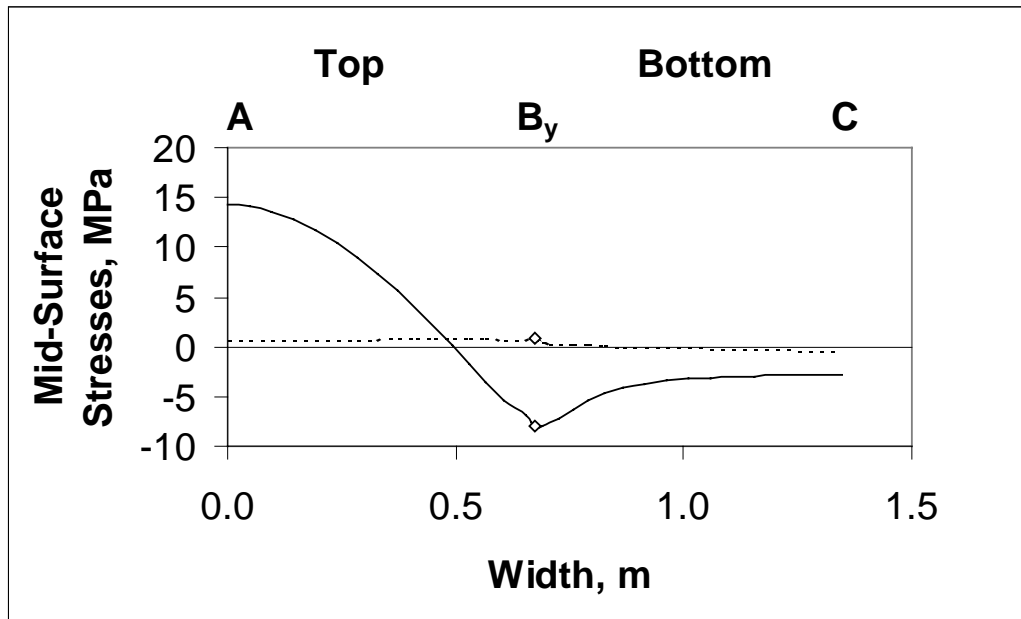
The mid-surface stresses along the X- and Y-axes are shown in Figure 4.2.3.1. The letters A, B_x, B_y, and C in the figure correspond to points shown in Figure 4.2.1.1. The open diamond in the plot signifies the edge of the tube. Mid-surface stress σ_{11} is denoted by a solid line, and σ_{22} is represented by a dashed line.

Figure 4.2.3.1a shows the mid-surface stresses along the X-axis. Mid-surface stress σ_{11} is constant and positive (tension) on the top surface of the tube until near the edge where it goes to zero. Stress σ_{11} is positive (tension) on the bottom in the region of uplift and gets close to zero at the center of the bottom surface. Mid-surface stress σ_{22} is zero everywhere along the tube except near the edge where it changes from being in tension to compression, back to tension, and into compression again at the edge. This is due to wrinkling. Mid-surface stress σ_{22} is positive (tension) in the region of uplift.

Figure 4.2.3.1.b shows the mid-surface stresses along the Y-axis. Stress σ_{11} is (positive) tension at the center of the top surface and is negative (compression) at the edge and on the bottom of the tube. Stress σ_{22} is almost zero along the entire cross section. Due to symmetry, the in-plane shear stresses along the X- and Y-axes are zero.



a: Along X-Axis



b: Along Y-Axis

Figure 4.2.3.1: Mid-Surface Stresses at a Pressure Head of 0.7m for $K_d = 4.20 \times 10^6$ N/m³ and $L_f:W_f$ of 5:1; σ_{11} solid, σ_{22} dashed

4.2.4 Pressure vs. Height

A pressure vs. height curve for a distributed spring stiffness, K_d , of $4.20 \times 10^6 \text{ N/m}^3$ is shown in Figure 4.2.4.1. Pressure heads ranging from 0.0m to 0.7m are plotted against the height of the tube, measured from the reference ground level $Z = 0$. The curve shows how the tube initially softens and then stiffens as the pressure increases.

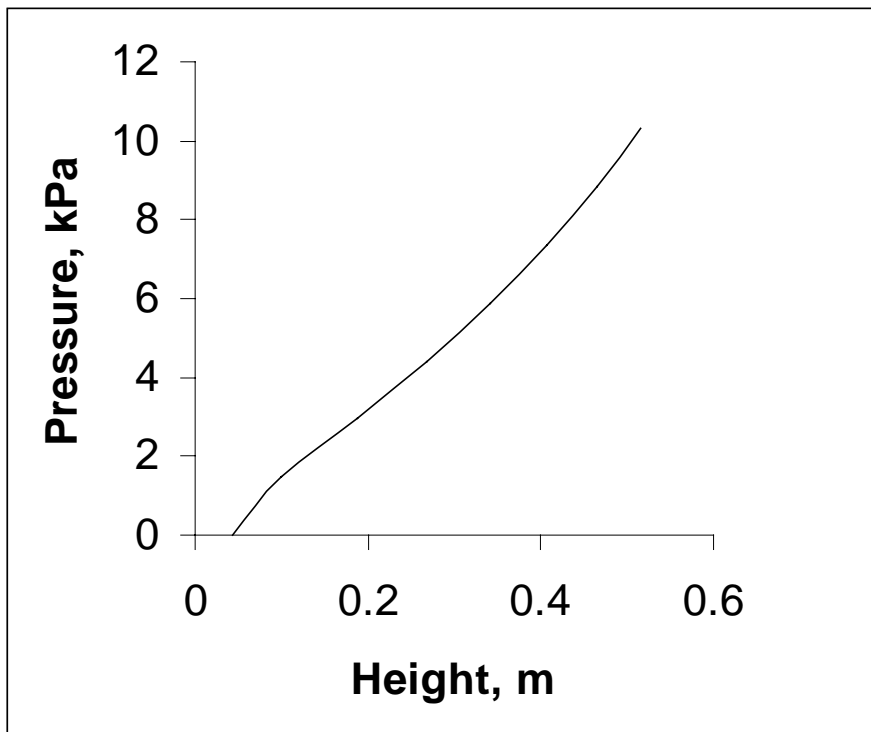


Figure 4.2.4.1: Pressure vs. Height for $K_d = 4.20 \times 10^6 \text{ N/m}^3$ and $L_f:W_f$ of 5:1

4.3 Distributed Spring Stiffness, K_d , of $8.40 \times 10^4 \text{ N/m}^3$

4.3.1 Geometry

One-quarter of the tube with a length-to-width ratio of 5:1 was modeled resting on tensionless springs with a distributed spring stiffness of $K_d = 8.40 \times 10^4 \text{ N/m}^3$, 50 times smaller than that used in the model discussed in Section 4.2. The maximum amount of hydrostatic pressure applied to this model at ground level was 5884 Pa, which equates to a pressure head of 0.4m.

Figure 4.3.1.1 shows a three-dimensional plot of this model. The top surface of the tube deflected upward 0.294m at its center from its initial height of 0.0429m. The bottom surface deflected downward 0.0949 m at its center from its initial height of 0.0m. The figure shows a small amount of wrinkling that occurred in the model.

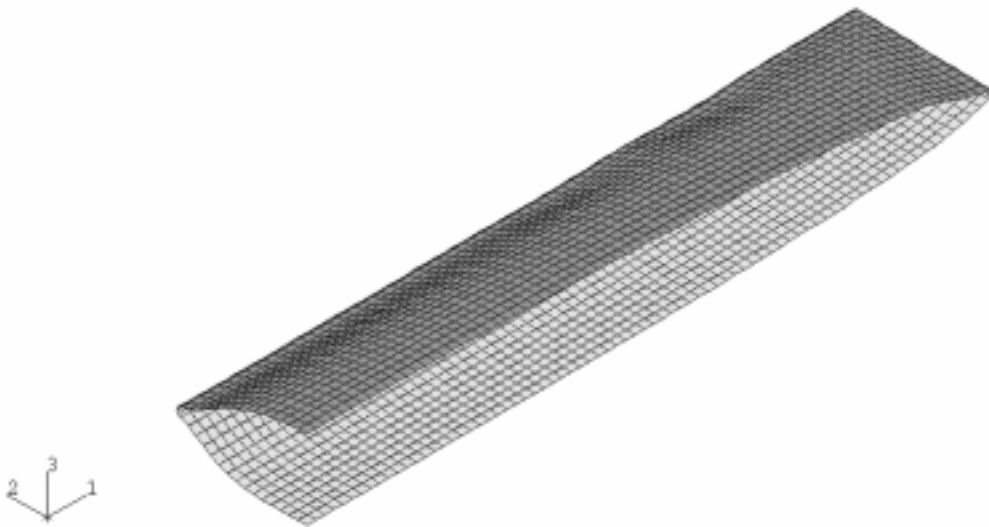
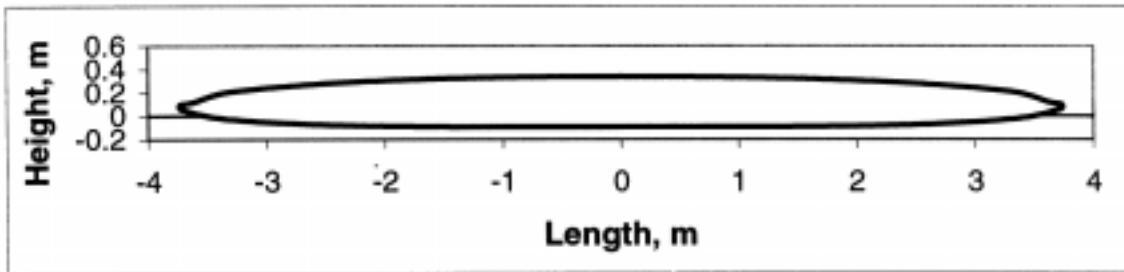
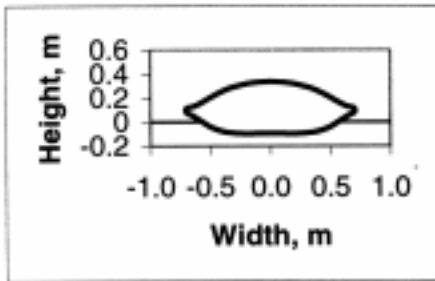


Figure 4.3.1.1: Pressure Head of 0.4m for $K_d = 8.40 \times 10^4 \text{ N/m}^3$ and $L_f:W_f$ of 5:1

Cross-sections of the model along the X- and Y-axes are shown in Figure 4.3.1.2. The coordinates of the tube's edge, in meters, at B_x , B_y , and the corner are (3.74, 0.0, 0.0825), (0.0, 0.707, 0.0980), and (3.74, 0.742, 0.0898), respectively.



a: Along X-Axis



b: Along Y-Axis

Figure 4.3.1.2: Cross Sections of the Tube at a Pressure Head of 0.4m for $K_d = 8.40 \times 10^4 \text{ N/m}^3$ and $L_f:W_f$ of 5:1

4.3.2 Contact Region

Figure 4.3.2.1 shows the contact region for one-quarter of the tube with an applied pressure head of 0.4m. The contact region for the entire tube at this pressure head is shown in Figure 4.3.2.2.

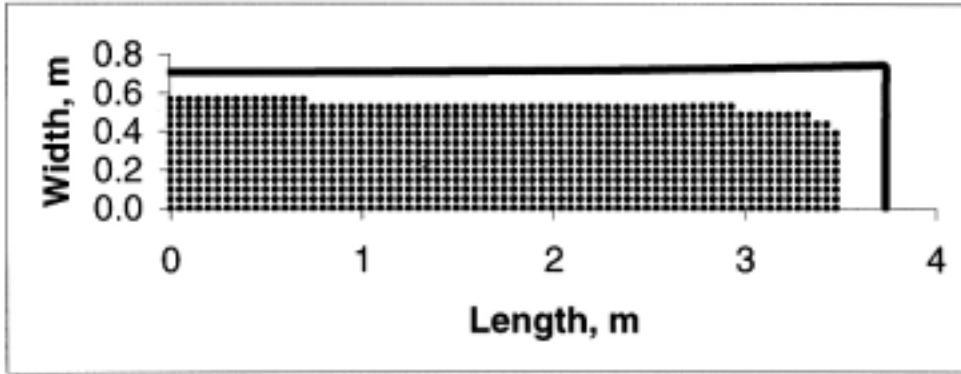


Figure 4.3.2.1: Quarter Contact Region at a Pressure Head of 0.4m for $K_d = 8.40 \times 10^4$ N/m^3 and $L_f:W_f$ of 5:1

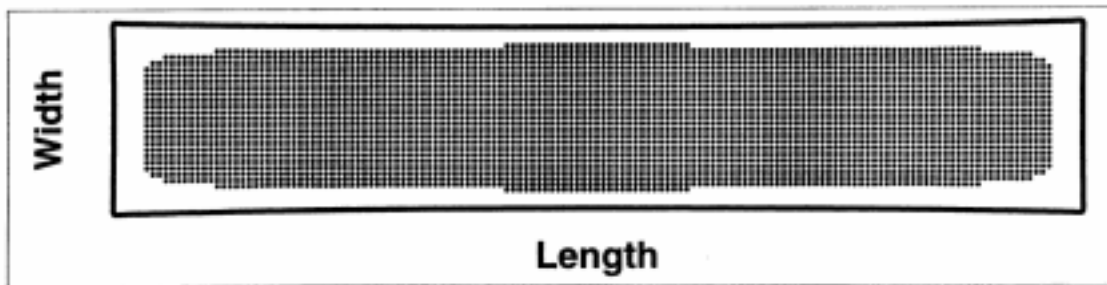
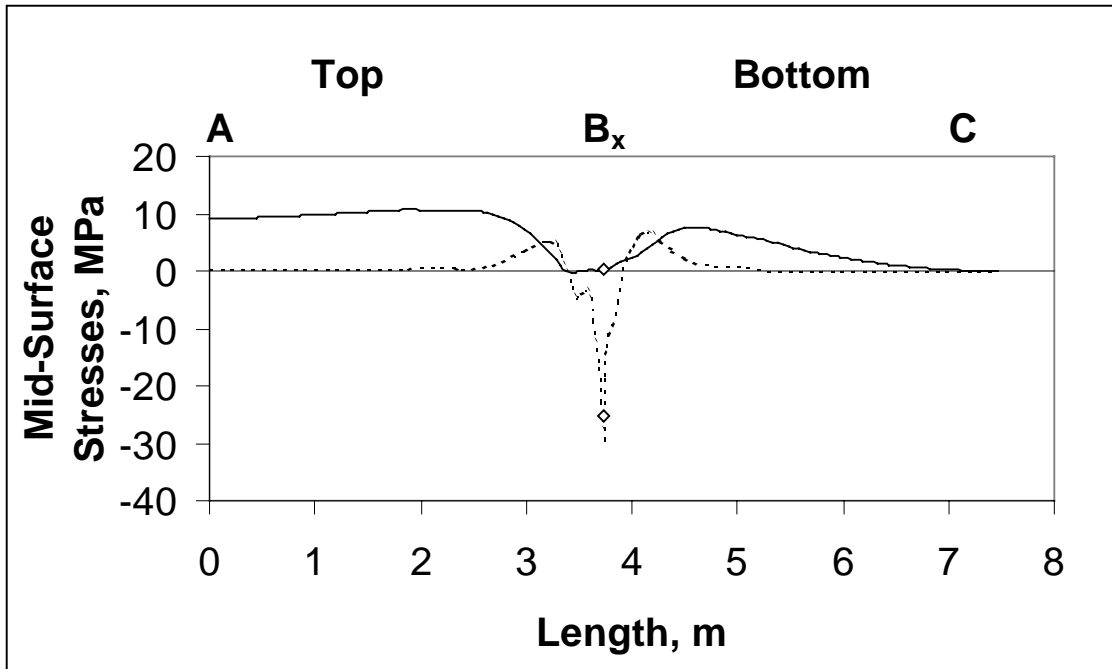


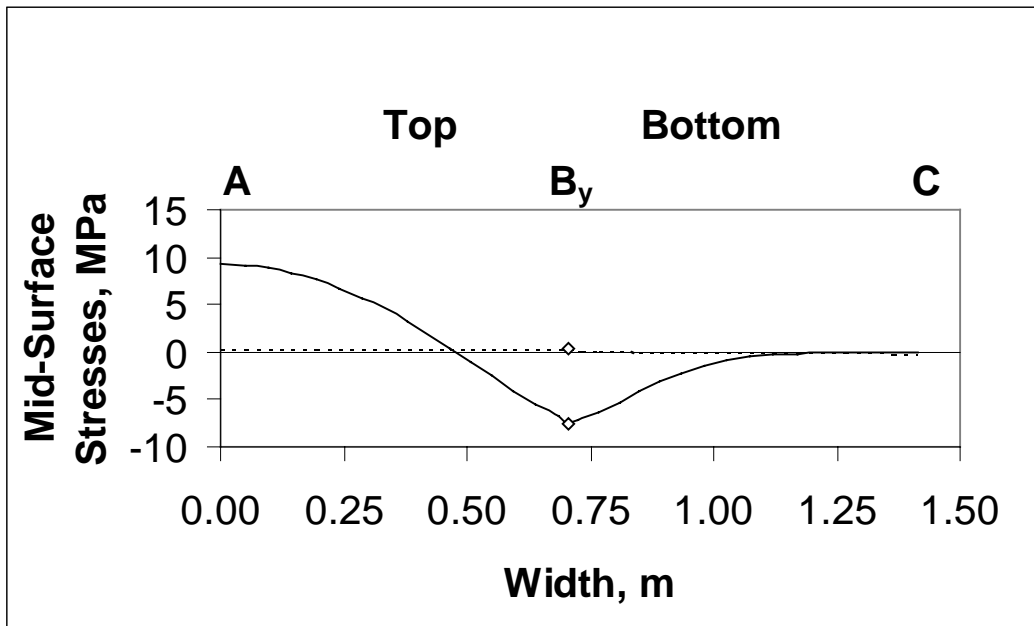
Figure 4.3.2.2: Whole Contact Region at a Pressure Head of 0.4m for $K_d = 8.40 \times 10^4$ N/m^3 and $L_f:W_f$ of 5:1

4.3.3 Mid-Surface Stresses

The mid-surface stresses along the X- and Y-axes are shown in Figure 4.3.3.1. Figure 4.3.3.1a shows the stresses along the X-axis. In this figure, in-plane mid-surface stress σ_{11} is positive (tension) and almost constant along the top surface of the tube except when it becomes zero near and at the edge. Stress σ_{11} is positive (tension) on the bottom and goes to zero at the center of the bottom surface. Mid-surface stress σ_{22} is zero everywhere except near the edge where it is positive (tension) and at the edge where it is negative (compression); this is due to wrinkling in the model.



a: Along X-Axis



b: Along Y-Axis

Figure 4.3.3.1: Mid-Surface Stresses at a Pressure Head of 0.4m for $K_d = 8.40 \times 10^4$ N/m^3 and $L_f:W_f$ of 5:1; σ_{11} solid, σ_{22} dashed

Figure 4.3.3.1b shows the mid-surface stresses along the Y-axis. Mid-surface stress σ_{11} on the top surface is positive (tension) near the center and negative (compression) at the edge. Near the center of the bottom surface of the tube, σ_{11} goes to zero. Mid-surface in-plane stress σ_{22} is either close to or is zero along the entire cross section. In-plane shear stresses along the X- and Y-axes are zero due to symmetry.

4.3.4 Pressure vs. Height

A pressure versus height curve is shown in Figure 4.3.4.1 for a tube with a length-to-width ratio of 5:1 and a distributed spring stiffness of $8.40 \times 10^4 \text{ N/m}^3$. The figure contains pressure heads ranging from 0.0m to 0.4m plotted against the corresponding tube height measured from the reference ground level of $Z = 0$. The curve shows how the tube initially softens at low pressures and stiffens as the pressure increases.

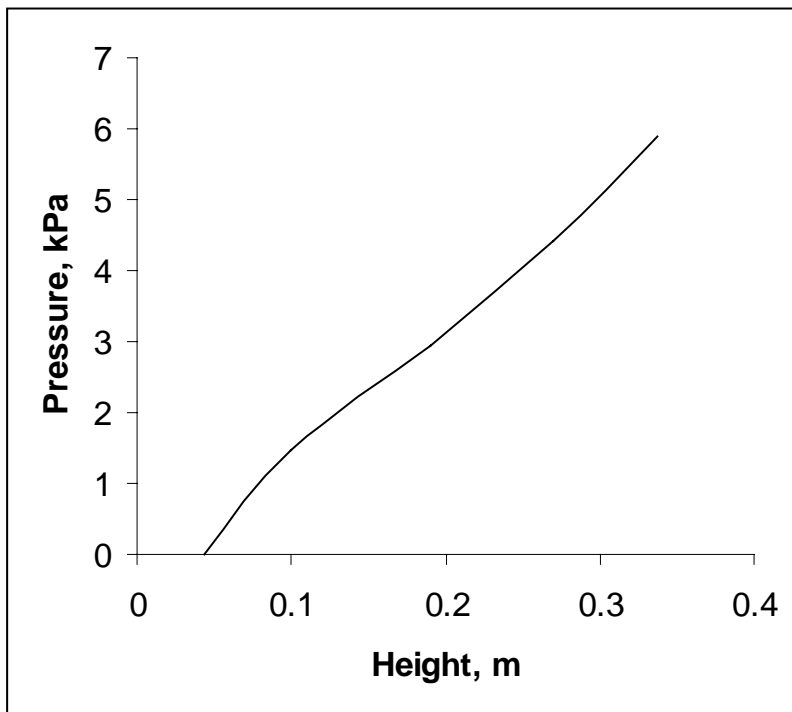


Figure 4.3.4.1: Pressure vs. Height for $K_d = 8.40 \times 10^4 \text{ N/m}^3$ and $L_f:W_f$ of 5:1

4.4 Discussion

The results obtained for the two distributed spring stiffnesses of $4.20 \times 10^6 \text{ N/m}^3$ and $8.40 \times 10^4 \text{ N/m}^3$ were compared for a tube with a length-to-width ratio of 5:1. The study showed that as the hydrostatic pressure increases, the contact region decreases. The stresses along the X- and Y-axes follow the same trend, although the mid-surface stresses for the distributed spring stiffness of $4.20 \times 10^6 \text{ N/m}^3$ along the X-axis appears to follow a sharper path than that for the distributed spring stiffness of $8.40 \times 10^4 \text{ N/m}^3$; this could be because a lower pressure was applied to the case with a distributed spring stiffness of $8.40 \times 10^4 \text{ N/m}^3$. The magnitudes for the distributed spring stiffness of $4.20 \times 10^6 \text{ N/m}^3$ are greater due to the greater amount of applied hydrostatic pressure.

Figure 4.4.1 shows the previous pressure vs. height plots for $K_d = 4.20 \times 10^6 \text{ N/m}^3$ and $K_d = 8.40 \times 10^4 \text{ N/m}^3$ plotted together. The line representing the pressure vs. height plot for $K_d = 4.20 \times 10^6 \text{ N/m}^3$ is dashed, and the line representing the plot for $K_d = 8.40 \times 10^4 \text{ N/m}^3$ is solid. Based upon this plot, for a tube with a length-to-width ratio of 5:1, the tube height, measured from the reference ground level $Z = 0$, does not appear to be influenced by the ground stiffness. If a larger amount of hydrostatic pressure were applied to the model with $K_d = 8.40 \times 10^4 \text{ N/m}^3$, the curve may diverge slightly and no longer overlap the results obtained for $K_d = 4.20 \times 10^6 \text{ N/m}^3$.

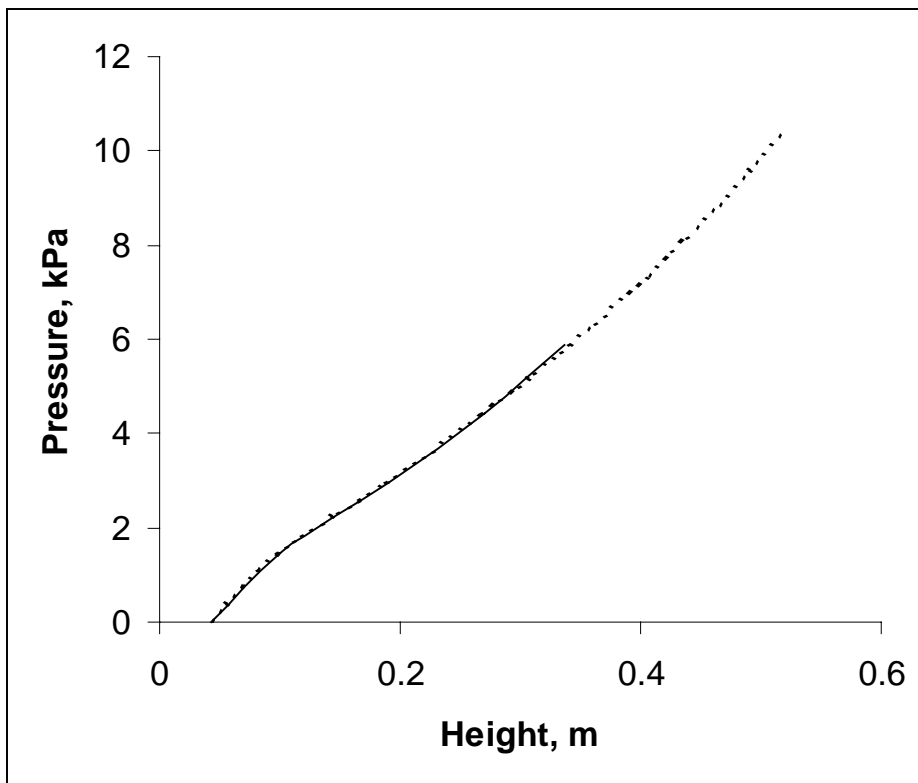


Figure 4.4.1: Pressure vs. Height for $K_d = 4.20 \times 10^6$ N/m³ (dashed) and $K_d = 8.40 \times 10^4$ N/m³ (solid) with $L_f:W_f$ of 5:1